

<b>Title</b>	Inversion in the In <sub>0.53</sub> Ga <sub>0.47</sub> As metal-oxide-semiconductor system: Impact of the In <sub>0.53</sub> Ga <sub>0.47</sub> As doping concentration
<b>Author(s)</b>	O'Connor, Éamon; Cherkaoui, Karim; Monaghan, Scott; Sheehan, Brendan; Povey, Ian M.; Hurley, Paul K.
<b>Publication date</b>	2017-01-19
<b>Original citation</b>	O'Connor, É., Cherkaoui, K., Monaghan, S., Sheehan, B., Povey, I. M. and Hurley, P. K. (2017) 'Inversion in the In <sub>0.53</sub> Ga <sub>0.47</sub> As metal-oxide-semiconductor system: Impact of the In <sub>0.53</sub> Ga <sub>0.47</sub> As doping concentration', Applied Physics Letters, 110, 032902 (5pp). doi:10.1063/1.4973971
<b>Type of publication</b>	Article (peer-reviewed)
<b>Link to publisher's version</b>	<a href="http://dx.doi.org/10.1063/1.4973971">http://dx.doi.org/10.1063/1.4973971</a> Access to the full text of the published version may require a subscription.
<b>Rights</b>	© 2017, the Authors. Reproduced with the permission of AIP Publishing from Applied Physics Letters, 110, 032902 (5pp). doi:10.1063/1.4973971 <a href="https://publishing.aip.org/authors/copyright-reuse">https://publishing.aip.org/authors/copyright-reuse</a>
<b>Item downloaded from</b>	<a href="http://hdl.handle.net/10468/4021">http://hdl.handle.net/10468/4021</a>

Downloaded on 2018-11-17T10:30:33Z

# 1                    **Inversion in the In<sub>0.53</sub>Ga<sub>0.47</sub>As Metal-Oxide-Semiconductor system:**

## 2                    **impact of the In<sub>0.53</sub>Ga<sub>0.47</sub>As doping concentration**

3                    É. O'Connor, K. Cherkaoui, S. Monaghan, B. Sheehan, I. M. Povey, and P. K. Hurley.

4                    <sup>1</sup>*Tyndall National Institute, University College Cork, Cork, Ireland.*

5                    *E-mail address of corresponding author: [eamonoconnor33@gmail.com](mailto:eamonoconnor33@gmail.com)*

6  
7 In<sub>0.53</sub>Ga<sub>0.47</sub>As metal-oxide-semiconductor (MOS) capacitors with Al<sub>2</sub>O<sub>3</sub> gate oxide and a range of *n* and *p*-  
8 type In<sub>0.53</sub>Ga<sub>0.47</sub>As epitaxial concentrations were examined. Multi-frequency capacitance-voltage and  
9 conductance-voltage characterization exhibited minority carrier responses consistent with surface  
10 inversion. The measured minimum capacitance at high frequency (1MHz) was in excellent agreement  
11 with the theoretical minimum capacitance calculated assuming an inverted surface. Minority carrier  
12 generation lifetimes,  $\tau_g$ , extracted from experimentally measured transition frequencies,  $\omega_m$ , using physics  
13 based a.c. simulations, demonstrated a reduction in  $\tau_g$  with increasing epitaxial doping concentration. The  
14 frequency scaled conductance,  $G/\omega$ , in strong inversion allowed the estimation of accurate  $C_{ox}$  values for  
15 these MOS devices.

16  
17  
18 Historically, a variety of issues have impeded progress for the incorporation of high-*k* dielectrics  
19 on III-V semiconductors for future CMOS applications.<sup>1,2</sup> Not least among these is the  
20 complexity of the high-*k* III-V interface which typically has a high density of electrically active  
21 defects.<sup>3,4,5</sup> Interface state density ( $D_{it}$ ) values in excess of  $10^{12}\text{cm}^{-2}$  are commonly reported  
22 which is almost two orders of magnitude higher than that achievable in SiO<sub>2</sub>/Si systems.  
23 Passivation of these defects to acceptable levels has not proved to be trivial and also renders  
24 reliable characterization and interpretation of device behavior difficult.<sup>6</sup> Such a high  $D_{it}$  can  
25 restrict Fermi level movement across the semiconductor bandgap and in the case of  
26 In<sub>0.53</sub>Ga<sub>0.47</sub>As, prevent surface inversion at the semiconductor/oxide interface. To date, only a  
27 limited number of studies in the literature have demonstrated sufficient reduction in  $D_{it}$  to allow  
28 the observation of true surface inversion and an associated minority carrier behavior, in the  
29 capacitance-voltage (CV) response of MOS capacitors on either *n*-type or *p*-type In<sub>0.53</sub>Ga<sub>0.47</sub>As.<sup>7,</sup>

30 8, 9, 10

31 In recent work we reported on a study of the minority carrier response of both  $n$ -type and  $p$ -  
32 type  $\text{In}_{0.53}\text{Ga}_{0.47}\text{As}$  metal-oxide-semiconductor (MOS) devices formed using an optimized 10%  
33 ammonium sulfide ( $(\text{NH}_4)_2\text{S}$ ) treatment.<sup>7</sup>  $D_{it}$  was sufficiently reduced such that a clear minority  
34 carrier response associated with inversion of the oxide/ $\text{In}_{0.53}\text{Ga}_{0.47}\text{As}$  surface was observed for  
35 both  $n$ -type and  $p$ -type devices. In order to extend this work, in this letter we present a method to  
36 confirm true surface inversion in  $\text{Al}_2\text{O}_3/\text{In}_{0.53}\text{Ga}_{0.47}\text{As}$  MOS capacitors based on the use of a wide  
37 range of  $n$  and  $p$ -type doping concentrations, ranging over two orders of magnitude from  
38  $\sim 1 \times 10^{16} \text{ cm}^{-3}$  to  $\sim 2 \times 10^{18} \text{ cm}^{-3}$ . This is in order to examine if the measured minimum capacitance  
39 scales correctly with the  $\text{In}_{0.53}\text{Ga}_{0.47}\text{As}$  doping concentration based on a maximum depletion  
40 width calculated assuming the surface is inverted. This follows an approach reported by  
41 Callegari *et al* for GaAs MOS devices.<sup>11</sup> In addition the effect of the doping concentration on the  
42 minority carrier generation lifetime in the  $\text{In}_{0.53}\text{Ga}_{0.47}\text{As}$ ,  $\tau_g$ , is examined. Finally, for these  
43 variable doping series samples, we utilize a recently reported method<sup>12</sup> to accurately estimate  
44 oxide capacitance,  $C_{ox}$ , where it was found that the peak magnitude of the angular frequency  
45 scaled conductance,  $G/\omega$ , was equal to  $C_{ox}^2/2(C_{ox}+C_D)$ , in strong inversion, where  $C_D$  is the  
46 semiconductor depletion capacitance.

47 The details of the  $\text{In}_{0.53}\text{Ga}_{0.47}\text{As}$  epitaxial layers used in this work are as follows. Firstly,  
48 using  $p$ -doped (Zn at  $\sim 2 \times 10^{18} \text{ cm}^{-3}$ )  $\text{InP}(100)$  as a starting substrate,  $\sim 2 \mu\text{m}$   $p$ - $\text{In}_{0.53}\text{Ga}_{0.47}\text{As}$  layers  
49 were grown by MOVPE with the following dopant (Zn) concentrations ( $\text{cm}^{-3}$ ):  $1.4 \times 10^{16}$ ,  
50  $3.3 \times 10^{16}$ ,  $1.8 \times 10^{17}$ ,  $2.7 \times 10^{17}$ , and  $2.0 \times 10^{18}$ . Using  $n$ -doped (S at  $\sim 2 \times 10^{18} \text{ cm}^{-3}$ )  $\text{InP}(100)$  as a  
51 starting substrate,  $\sim 2 \mu\text{m}$   $n$ - $\text{In}_{0.53}\text{Ga}_{0.47}\text{As}$  layers were grown by MOVPE with the following  
52 dopant (Si) concentrations ( $\text{cm}^{-3}$ ):  $7.8 \times 10^{15}$ ,  $3.0 \times 10^{16}$ ,  $2.0 \times 10^{17}$ ,  $6.0 \times 10^{17}$ , and  $2.0 \times 10^{18}$ . These  
53 doping concentrations were determined by Electrochemical Capacitance-Voltage (ECV)  
54 Profiling.  $\text{In}_{0.53}\text{Ga}_{0.47}\text{As}$  surfaces were initially rinsed for 1 minute each in acetone, methanol,  
55 and isopropanol, immediately followed by immersion for 20 minutes at room temperature in  
56  $(\text{NH}_4)_2\text{S}$  with a concentration of 10% in deionised  $\text{H}_2\text{O}$ . These optimized passivation parameters  
57 were determined from previous physical and electrical studies<sup>13,14</sup> and subsequently also reported  
58 for MOSFET devices.<sup>15</sup> The  $\text{Al}_2\text{O}_3$  layers were grown by atomic layer deposition (ALD) at  
59  $300^\circ\text{C}$  (Cambridge NanoTech, Fiji F200LLC), using alternating pulses of TMA ( $\text{Al}(\text{CH}_3)_3$ ) and  
60  $\text{H}_2\text{O}$ . TEM indicated an  $\text{Al}_2\text{O}_3$  thickness of  $\sim 7 \text{ nm}$  for the growth run on  $p$ -type samples and a  
61 thickness of  $\sim 5 \text{ nm}$  for the separate ALD growth run on  $n$ -type samples. Finally, gate contacts  $\sim$

62 160 nm thick were formed by e-beam evaporation of Ni (70nm), and Au (90nm), using a lift-off  
 63 process. Electrical measurements were recorded using an Agilent E4980A, and were performed  
 64 on-wafer in a microchamber probe station (Cascade, Summit 12971B) in a dry air, dark  
 65 environment (dew point  $\leq 203\text{K}$ ).

66 For an MOS device in strong inversion the depletion layer width reaches a maximum  
 67 value, which is related to the doping concentration and the relative permittivity of the  
 68 semiconductor.<sup>16</sup> The equation governing the maximum depletion width, included here for  
 69 completeness, is given in Equation [1] below where:  $\epsilon_0$  is the permittivity of free space;  $\epsilon_s$  is the  
 70 semiconductor permittivity;  $k$  is Boltzmann's constant;  $n_i$  is the intrinsic semiconductor carrier  
 71 concentration;  $N_D$  is the semiconductor doping concentration.<sup>17</sup>

$$72 \quad x_{d\_max} = \sqrt{\frac{4\epsilon_0\epsilon_s kT \ln(N_D/n_i)}{q^2 N_D}} \quad [1]$$

73 From this equation, as the semiconductor doping level is increased this maximum depletion  
 74 width is reduced, which in turn is reflected in an increase in the depletion capacitance ( $C_D$ ) of the  
 75 semiconductor in inversion. The theoretical minimum capacitance ( $C_{\text{min-theor}}$ ) of a gate stack is  
 76 the series combination of  $C_D$  and  $C_{\text{ox}}$ . It is thus expected that for an inverted surface, the  
 77 minimum measured gate stack capacitance ( $C_{\text{min-meas}}$ ) will increase as a function of doping  
 78 concentration. Utilizing different doping concentrations  $C_{\text{min-meas}}$  at high frequency can be  
 79 compared with  $C_{\text{min-theor}}$  as calculated by assuming the semiconductor surface is inverted. In the  
 80 case of devices where the  $D_{\text{it}}$  is high, Fermi level movement will be restricted such that it will not  
 81 be possible to reach the minimum capacitance. Where substrates with variable doping levels are  
 82 available this provides a means to investigate if the oxide-semiconductor interface state  
 83 concentration has been reduced to levels which allow surface inversion to be achieved. This  
 84 approach was used previously for GaAs MOS structures to investigate improvements in the CV  
 85 characteristics of plasma deposited Ga oxide films on GaAs substrates.<sup>11</sup>

86 Figure 1(a) plots the 1 MHz CV responses for the  $p$ -type  $\text{In}_{0.53}\text{Ga}_{0.47}\text{As}$  MOS devices with  
 87 varying dopant concentrations. The 1 MHz curves were chosen in order to minimize any  
 88 contribution of interface states to the measured CV response. Open symbols represent  $C_{\text{min-theor}}$   
 89 for each doping concentration and calculated using a  $C_{\text{ox}}$  value in this case of  $0.0075 \text{ F/m}^2$ , taken

90 from the measured capacitance at low frequency (20 Hz), and at a gate bias of 1.75V.  $C_{ox}$  was  
91 chosen at 20Hz as this was the lowest frequency that could be measured with the instrument  
92 used, and previous work has shown that the CV at 20Hz provides a very close approximation to  
93 the  $C_{ox}$  obtained using a quasi-static CV.<sup>18</sup> It is clear that the measured minimum capacitance  
94 increases as expected with doping and that there is excellent agreement between the measured  
95 and theoretical minimum capacitance values, providing strong evidence that the  $In_{0.53}Ga_{0.47}As$   
96 surface is inverted. This is notable considering that the change in doping concentration is over  
97 two orders of magnitude. It is also significant that the measured CV curves go flat with  
98 increasing positive gate bias, which is further support that  $D_{it}$  has been reduced to an extent to  
99 allow sufficient Fermi level movement that permits surface inversion. Figure 1(b) shows the 1  
100 MHz CV responses for the  $n$ -type  $In_{0.53}Ga_{0.47}As$  MOS devices with changing epitaxial layer  
101 dopant concentrations. As in the case of the  $p$ -type samples, there is excellent agreement between  
102 the measured (open symbols) and theoretical (closed symbols) capacitance values. The  
103 theoretical minimum capacitance,  $C_{min-theor}$ , for each doping concentration was calculated using a  
104  $C_{ox}$  value in this case of  $0.0093 \text{ F/m}^2$ , taken from the capacitance measured at low frequency  
105 (20Hz), and at a gate bias of -3.75V. When plotting the measured capacitance versus the  
106 theoretical value, (@1.75  $V_{gate}$  for  $p$ -type and at @-3.75 $V_{gate}$  for  $n$ -type), Figure 2 demonstrates  
107 that there is close to a linear relationship in both cases. The inversion of the  $n$ -type  $In_{0.53}Ga_{0.47}As$   
108 MOS is of particular note, as for the  $Al_2O_3/In_{0.53}Ga_{0.47}As$  MOS system the interface state density  
109 is generally reported to rise steeply towards the valence band edge,<sup>19,20,21</sup> and the ability to invert  
110 the  $Al_2O_3/n$ - $InGaAs$  surface indicates that the surface preparation and ALD growth conditions  
111 have not only reduced  $D_{it}$  near the mid gap energy, but also results in  $D_{it}$  reduction from mid-gap  
112 to the valence band edge.

113 For all samples the multi-frequency CV and GV responses (20 Hz to 1 MHz) also exhibited the  
114 characteristic signatures of inversion behavior for  $In_{0.53}Ga_{0.47}As$  MOS devices.<sup>7</sup> As an example  
115 illustration the CVs in Figure 3(a) and (b) are plotted for the devices in this study ( $1.8 \times 10^{17} p$ -  
116 type and  $6.0 \times 10^{17} n$ -type) having doping levels similar to those used in previous reports on  
117 inverted  $In_{0.53}Ga_{0.47}As$  MOS devices, in order to show the behavior is consistent.<sup>7,22</sup> Space  
118 limitations preclude showing the multi-frequency CV for all samples. One of the signatures for  
119 an inverted surface is that in strong inversion the measured conductance normalized by

120 frequency,  $G/\omega$ , peaks at the transition frequency,  $\omega_m$ .<sup>7,12,23</sup> This relationship is observed for all  
121 samples in the study (not shown).

122 For an inverted surface the multi-frequency C-V and G-V responses can also be used to  
123 investigate the minority carrier lifetime in the  $\text{In}_{0.53}\text{Ga}_{0.47}\text{As}$  layer and the capacitance of the gate  
124 oxide.<sup>12,22</sup> For the case of surface inversion, the transition frequency,  $\omega_m$ , is inversely related to  
125 the minority carrier generation lifetime,  $\tau_g$ , in the  $\text{In}_{0.53}\text{Ga}_{0.47}\text{As}$ , and the peak value of  $G/\omega$  is  
126 related to the oxide capacitance,  $C_{\text{ox}}$ . Considering firstly the case of the minority carrier lifetime,  
127 the  $G/\omega$  recorded at a gate bias of  $1.75 V_{\text{gate}}$  for  $p$ -type and at  $-3.75V_{\text{gate}}$  for  $n$ -type are plotted in  
128 Figure 4. One observation of note over both  $n$  and  $p$ -type samples in Figure 4 is that the  
129 transition frequency at which  $G/\omega$  peaks in inversion increases as the semiconductor doping  
130 concentration is increased. Figure 5(a) plots this change for  $p$ -type and  $n$ -type devices. For a  
131 minority carrier supply provided through mid-gap state generation, this behavior is expected as  
132 the minority carrier lifetime  $\tau_g$  values generally decrease with increasing doping concentration.  
133 These observations are therefore consistent with previous work on similar device structures  
134 indicating that at room temperature the dominant mechanism for the supply of minority carriers  
135 is a generation-recombination process through mid-gap bulk defects in the  $\text{In}_{0.53}\text{Ga}_{0.47}\text{As}$   
136 depletion region.<sup>7</sup> These results are not consistent with a border trap<sup>24</sup> contribution to the  
137 observed minority carrier response. The results in Figure 5(a) also indicate that at similar doping  
138 levels the transition frequency for the  $n$ -type samples is generally one order of magnitude higher  
139 than for the corresponding  $p$ -type samples.

140 A Synopsis Sentaurus device simulator was employed to perform physics based ac simulations,  
141 where the value of  $\tau_g$  in the simulations is altered to achieve a match between the transition  
142 frequency of the physics based ac simulations and the experimental transition frequency values  
143 in Figure 5(a). The resulting  $\tau_g$  are plotted in Figure 5(b) demonstrating a marked decrease with  
144 increasing doping concentration for both  $n$  and  $p$ -type devices. The fact that higher generation  
145 lifetimes at similar doping levels are observed for  $p$ -type compared to  $n$ -type samples is possibly  
146 related to inequalities in the bulk  $\text{In}_{0.53}\text{Ga}_{0.47}\text{As}$  properties arising from differences in the  
147 epitaxial growth conditions for the  $p$  and  $n$ -type  $\text{In}_{0.53}\text{Ga}_{0.47}\text{As}$  layers. However, further analysis  
148 of this is beyond the scope of the current study. Previous work also demonstrated that it is  
149 possible to passivate some of the bulk mid-gap traps in  $\text{In}_{0.53}\text{Ga}_{0.47}\text{As}$  through  $\text{H}_2/\text{N}_2$  annealing,

150 as indicated by an increase in  $\tau_g$ .<sup>22,25</sup> It is noted that all samples in each doping series in this work  
151 were processed simultaneously with the  $\text{In}_{0.53}\text{Ga}_{0.47}\text{As}$  surface seeing identical conditions and  
152 therefore should have comparable  $D_{it}$ . Interface states do not contribute to the observed minority  
153 carrier response because in strong inversion interface states are either full ( $p$ -type) or empty ( $n$ -  
154 type). Therefore changes in surface potential arising from modulation of the small signal a.c.  
155 voltage applied to the gate will not significantly affect their occupancy.<sup>22</sup>

156  $C_{ox}$  is an important parameter in device analysis, for example with regard to  $D_{it}$  extraction.  
157 These doping series samples can also be utilized with regard to the  $C_{ox}$  extraction method we  
158 published recently,<sup>12</sup> where it was demonstrated that in strong inversion the maximum value of  
159  $G/\omega$  at  $\omega_m$  is equal to  $C_{ox}^2/2(C_{ox}+C_D)$ . In the current study the oxide thickness is fixed while the  
160 doping concentration is varied. Therefore, for a given  $C_{ox}$ , as doping concentration increases,  $C_D$   
161 will increase and it would be expected using the above relationship that the value of  $G/\omega$  would  
162 decrease. Figure 6 plots the expected theoretical values of  $G/\omega$  versus doping, for various values  
163 of  $C_{ox}$ . The measured  $G/\omega$  values are plotted as open symbols, with the dashed blue lines  
164 representing an approximate fitting to those points in each case. It is seen that the experimental  
165 values follow the trend of the theoretical values quite closely. In Figure 6 (a) it is evident that the  
166 curve calculated using  $C_{ox}$  of  $0.0075 \text{ F/m}^2$  is in very good agreement with the experimental  $G/\omega$   
167 data. In the case of the  $n$ -type devices the  $0.0093 \text{ F/m}^2$  for  $C_{ox}$  provides a good approximation  
168 over most of the doping range, although some deviation is observed in the experimental data for  
169 the two highest doping concentrations. These observations are important also in validating the  
170 calculations of the theoretical minimum capacitances described earlier in regard to Figure 1 and  
171 2, where the  $C_{ox}$  values used to extract the theoretical minimum capacitances were  $0.0075 \text{ F/m}^2$   
172 and  $0.0093 \text{ F/m}^2$  for  $p$ -type and  $n$ -type samples respectively, determined from the measured  
173 capacitance at 20Hz. Therefore the  $C_{ox}$  values that provide the best fit in both  $n$  and  $p$ -type cases  
174 in Figure 6 are in agreement with the  $C_{ox}$  measured at low frequency (20Hz).

175 In summary,  $p$ -type and  $n$ -type  $\text{Au/Ni/Al}_2\text{O}_3/\text{In}_{0.53}\text{Ga}_{0.47}\text{As}$  MOS capacitors with  
176 semiconductor doping concentrations ranging from  $10^{16}\text{cm}^{-3}$  to  $10^{18}\text{cm}^{-3}$  exhibited behavior  
177 consistent with surface inversion. The measured minimum capacitance at 1 MHz scales correctly  
178 with the  $\text{In}_{0.53}\text{Ga}_{0.47}\text{As}$  doping concentration based on a maximum depletion width calculated  
179 assuming the surface is inverted, providing evidence that the interface state concentration was

180 reduced to a level which allows inversion of the  $\text{Al}_2\text{O}_3/\text{In}_{0.53}\text{Ga}_{0.47}\text{As}$  interface for both  $n$  and  $p$   
181 type doped  $\text{In}_{0.53}\text{Ga}_{0.47}\text{As}$ . The minority carrier generation lifetime in the  $\text{In}_{0.53}\text{Ga}_{0.47}\text{As}$ ,  $\tau_g$ , was  
182 found to decrease with increasing doping concentration.  $C_{\text{ox}}$  values extracted using a method  
183 based on the relationship between the capacitance and conductance in strong inversion exhibited  
184 excellent agreement with the  $C_{\text{ox}}$  measured at low frequency (20 Hz). It is notable that this was  
185 illustrated previously using an  $\text{Al}_2\text{O}_3$  thickness series on both  $n$  and  $p$ -type  $\text{In}_{0.53}\text{Ga}_{0.47}\text{As}$  in  
186 which case the doping was fixed and  $C_{\text{ox}}$  varied with dielectric thickness<sup>22</sup>, and also that results  
187 from physics based a.c simulations show the relationship to be generally true.<sup>12</sup> Those results,  
188 combined with the results of this variable doping study, indicate that the equality of the  
189 maximum value of  $G/\omega$  at  $\omega_m$  being equal to  $C_{\text{ox}}^2/2(C_{\text{ox}}+C_D)$  in inversion, is a reliable tool to  
190 obtain an accurate estimate of  $C_{\text{ox}}$ , and most significantly that this method can be applied for any  
191 MOS system in inversion, regardless of the oxide or semiconductor material.

192

193 The authors acknowledge the following colleagues from Tyndall National Institute for their  
194 contribution: Dr. Kevin Thomas and Dr. Emanuele Pelucchi for MOVPE growth; Dr. Pat  
195 Carolan for TEM analysis, and Dan O’Connell for lithography and gate metallization. The  
196 authors acknowledge Dr. Rafael Rios (retired) formerly of Intel Components Research, Oregon,  
197 for providing the physics based CV simulations. This work was supported in part by Science  
198 Foundation Ireland under the “INVENT” project 09/IN.1/I2633; and in part by the European  
199 Commission through the project entitled “Compound Semiconductors for 3D Integration  
200 COMPOSE3” under Grant FP7-ICT-2013-11-619325; and the project entitled “Integration of III-  
201 V Nanowire Semiconductors for Next Generation High Performance CMOS SOC Technologies,  
202 (INSIGHT)” under Grant H2020-ICT-2015-688784. É. O’Connor acknowledges the financial  
203 support of the European Union funded Marie Curie fellowship “FACIT” (FP7-PEOPLE-2013-  
204 IEF 628523).

205



206

207 Figure 1. 1MHz CV responses at 295K for (a) Au/Ni/7nm-Al<sub>2</sub>O<sub>3</sub>/*p*-In<sub>0.53</sub>Ga<sub>0.47</sub>As and (b)  
208 Au/Ni/5nm-Al<sub>2</sub>O<sub>3</sub>/*n*-In<sub>0.53</sub>Ga<sub>0.47</sub>As MOS devices with dopant concentrations ranging from ~ 10<sup>16</sup>  
209 cm<sup>-3</sup> to 10<sup>18</sup> cm<sup>-3</sup>. The theoretical values (open symbols) were estimated using a C<sub>ox</sub> value of  
210 0.0075 F/m<sup>2</sup>, and 0.0093 F/m<sup>2</sup> for the *p*- and *n*-type devices respectively.

211

212 Figure 2. Plot of measured versus theoretical minimum capacitance for: (a) different *p*-type  
213 doping concentrations, with the measured values being those at a gate bias of 1.75 V in Fig. 1(a);  
214 and (b) different *n*-type doping concentrations, with the measured values being those at a gate  
215 bias of -3.75 V in Figure 1(b).

216

217 Figure 3: Multi-frequency CV responses at 295K of (a) *p*-type and (b) *n*-type  
218 Au/Ni/Al<sub>2</sub>O<sub>3</sub>/In<sub>0.53</sub>Ga<sub>0.47</sub>As, devices, with In<sub>0.53</sub>Ga<sub>0.47</sub>As doping concentrations of 2.7x10<sup>17</sup> cm<sup>-3</sup>  
219 and 6.0x10<sup>17</sup> cm<sup>-3</sup>, and Al<sub>2</sub>O<sub>3</sub> thicknesses of ~ 7 nm and 5 nm, respectively. The CV responses  
220 with increasing positive gate bias for the *p*-type devices, and with increasing negative gate bias  
221 for the *n*-type devices, are consistent with the CV behavior arising from a minority carrier  
222 response in inversion.

223

224 Figure 4. G<sub>m</sub>/ω plotted versus ω in strong inversion for (a) Au/Ni/7nm Al<sub>2</sub>O<sub>3</sub>/*p*-In<sub>0.53</sub>Ga<sub>0.47</sub>As,  
225 and (b) Au/Ni/5nm Al<sub>2</sub>O<sub>3</sub>/*n*-In<sub>0.53</sub>Ga<sub>0.47</sub>As devices. The values of G/ω were taken at a gate bias  
226 of 1.75 V for *p*-In<sub>0.53</sub>Ga<sub>0.47</sub>As devices and at a gate bias of -3.75 V for *n*-In<sub>0.53</sub>Ga<sub>0.47</sub>As devices,  
227 utilizing the multi-frequency GV data. Note, the frequency scaled conductance, G/ω, can also be  
228 expressed in units of F/m<sup>2</sup>.

229

230 Figure 5. (a) Increase in transition frequency, ω<sub>m</sub>, as a function of In<sub>0.53</sub>Ga<sub>0.47</sub>As doping  
231 concentration for *p*-type (star) and *n*-type (circle) MOS devices. (b) Decrease in the minority

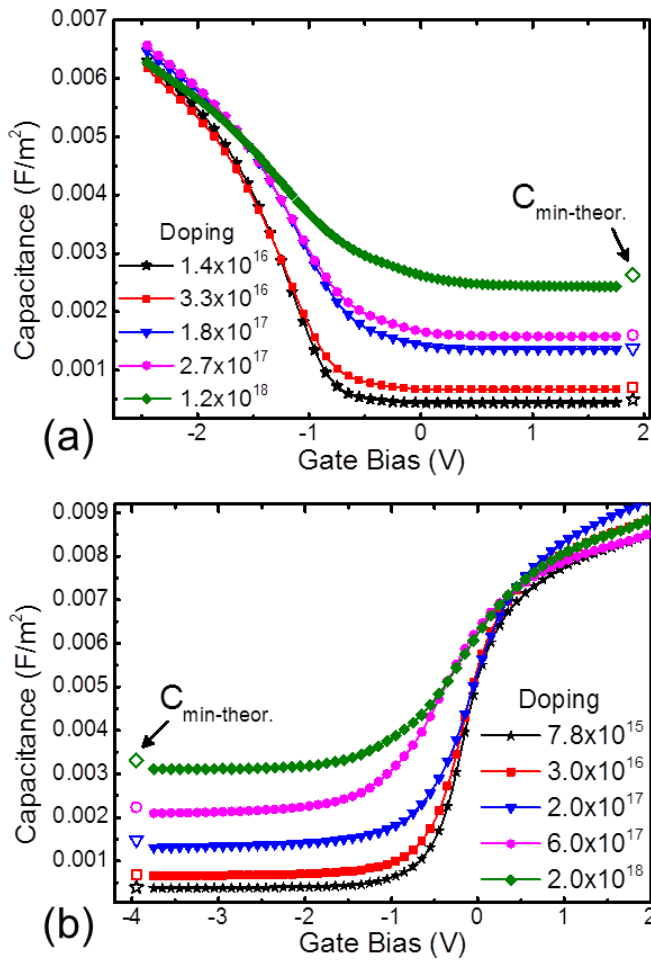
232 carrier generation lifetime,  $\tau_g$ , with increasing doping for  $p$ -type (star) and  $n$ -type (circle) MOS  
 233 devices.

234

235 Figure 6. Peak  $G/\omega$  in inversion as a function of doping concentration for (a)  $p$ -type and (b)  $n$ -  
 236 type Au/Ni/Al<sub>2</sub>O<sub>3</sub>/In<sub>0.53</sub>Ga<sub>0.47</sub>As devices. Different  $C_{ox}$  values were used to compute the  
 237 corresponding theoretical  $G/\omega$  values at each doping level according to the  
 238  $(G/\omega)_{max}=C_{ox}^2/2(C_{ox}+C_D)$  relationship. The measured peak  $G/\omega$  values in strong inversion are  
 239 plotted as open symbols, and fitted with the dashed line. Note, the frequency scaled conductance,  
 240  $G/\omega$ , can also be expressed in units of F/m<sup>2</sup>.

241

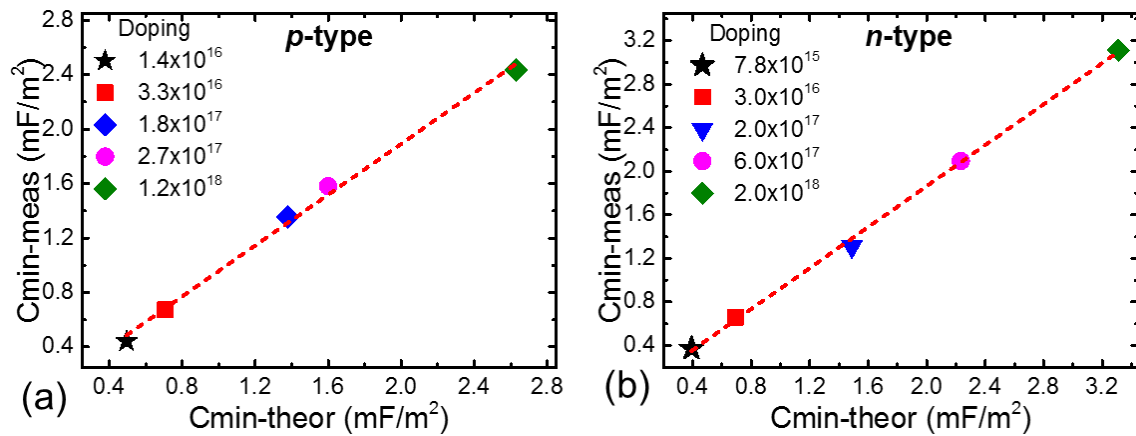
242 Figure 1



243

244

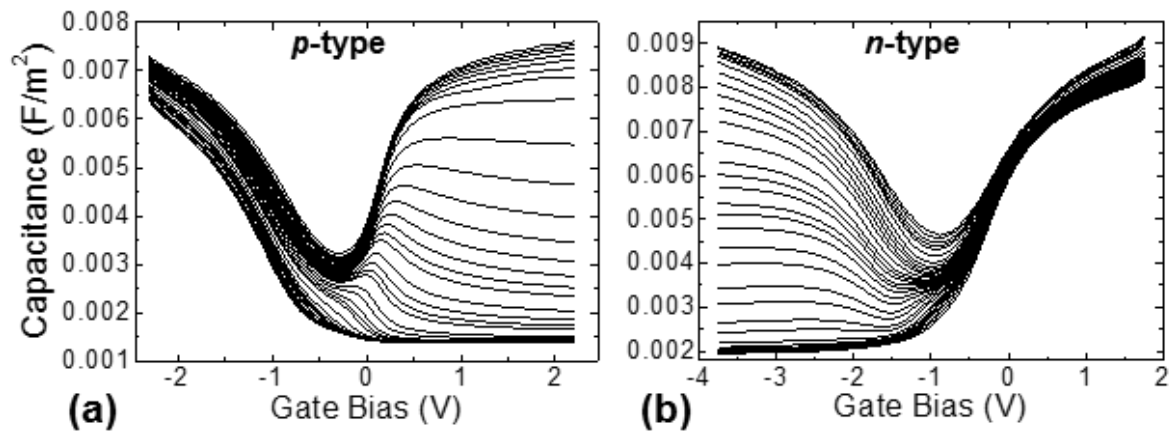
245 Figure 2



246

247

248 Figure 3



249

250

251

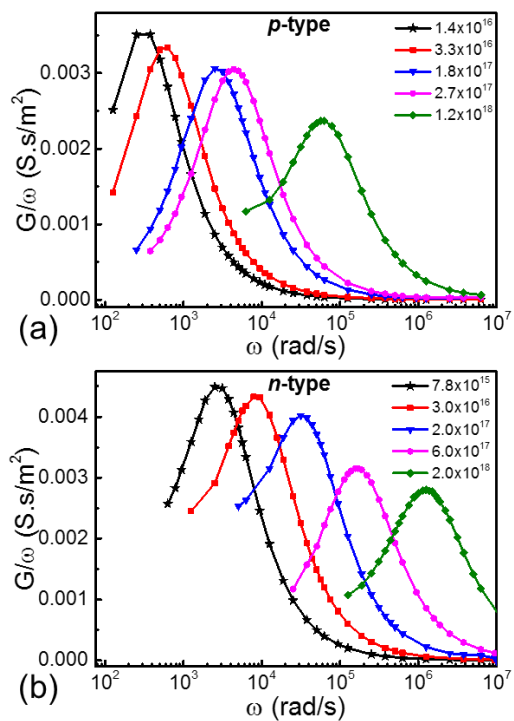
252

253

254

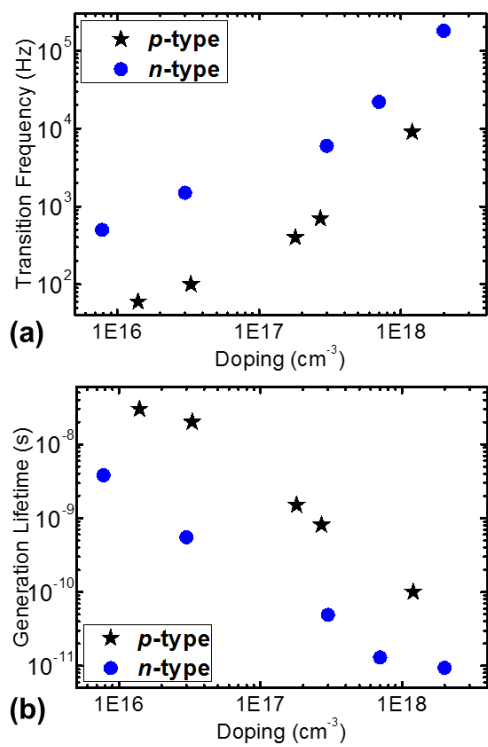
255

256 Figure 4



257

258 Figure 5

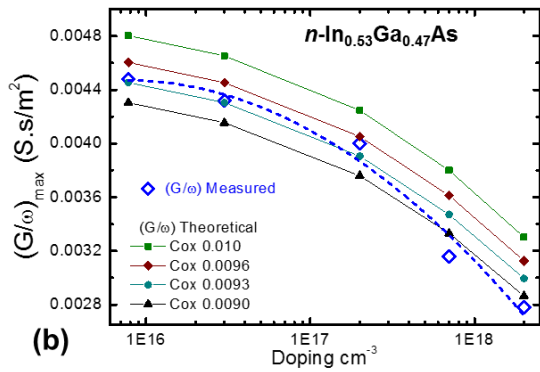
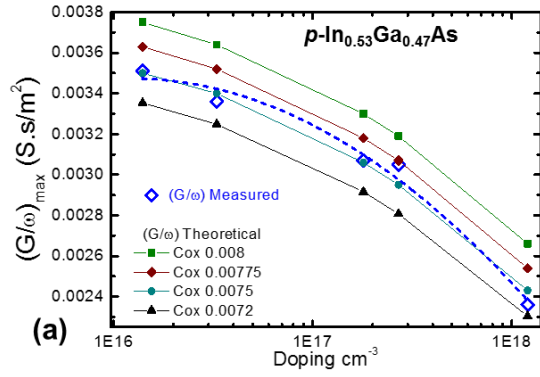


259

260

261

262 Figure 6



263

264

- 
- <sup>1</sup> J. Del Alamo, *Nature*, **479**, 317 (2011).
- <sup>2</sup> I. Thayne, S. Bentley, M. Holland, W. Jansen, X. Li, D. Macintyre, S. Thom, B. Shin, J. Ahn, P. McIntyre, *Microelec. Eng.*, **88**, 1070 (2011).
- <sup>3</sup> C. L. Hinkle, E. M. Vogel, P. D. Ye R. M. Wallace, *Curr. Opin. Sol. State Mat. Sci.* **15**, 188 (2011).
- <sup>4</sup> H.-P. Komsa, A. Pasquarello, *Microelec. Eng.*, **88**, 1436 (2011).
- <sup>5</sup> J. Robertson, Y. Guo, and L. Lin, *J. Appl. Phys.*, **117**, 112806 (2015).
- <sup>6</sup> R. Engel-Herbert, Y. Hwang, and S. Stemmer, *J. Appl. Phys.*, **108**, 124101 (2010).
- <sup>7</sup> E. O'Connor, S. Monaghan, K. Cherkaoui, I. M. Povey, and P. K. Hurley, *Appl. Phys. Lett.*, **99**, 212901, (2011).
- <sup>8</sup> H. C. Lin, W-E. Wang, G. Brammertz, M. Meuris, and M. Heyns, *Microelec. Eng.*, **86** 1554 (2009)
- <sup>9</sup> H. D. Trinh, E. Y. Chang, P. W. Wu, Y. Y. Wong, C. T. Chang, Y. F. Hsieh, C. C. Yu, H. Q. Nguyen, Y. C. Lin, K. L. Lin, and M. K. Hudait, *Appl. Phys. Lett.*, **97**, 042903 (2010).
- <sup>10</sup> T. D. Lin, Y. H. Chang, C. A. Lin, M. L. Huang, W. C. Lee, J. Kwo, and M. Hong, *Appl. Phys. Lett.*, **100**, 172110 (2012).
- <sup>11</sup> A. Callegari, P. D. Hoh, D. A. Buchanan, and D. Lacey, *Appl. Phys Lett.*, **54**, 332 (1989).
- <sup>12</sup> S. Monaghan É. O'Connor, R. Rios, F. Ferdousi, Liam Floyd, E. Ryan, K. Cherkaoui, I. M. Povey, K. J. Kuhn, and P. K. Hurley, *IEEE Trans .Elec. Dev .*, **61**. 4176, (2014).
- <sup>13</sup> É. O'Connor B Brennan, V Djara, K Cherkaoui, S Monaghan, SB Newcomb, R Contreras, M Milojevic, G Hughes, ME Pemble, RM Wallace, PK Hurley, *J. Appl. Phys.*, **109**, 024101 (2011).
- <sup>14</sup> B. Brennan, M. Milojevic, C. L. Hinkle, F. S. Aguirre-Tostado, G. Hughes, and R. M. Wallace, *Appl. Surf. Sci.*, **257** 4082–4090 (2011).
- <sup>15</sup> J. J. Gu, A. T. Neal, and P. D. Ye, *Appl. Phys. Lett.*, **99**, 152113 (2011).
- <sup>16</sup> S. M. Sze, “*Physics of Semiconductor Devices*”, J. Wiley & Sons, (1981).
- <sup>17</sup> The In<sub>0.53</sub>Ga<sub>0.47</sub>As permittivity and intrinsic carrier concentration parameters were taken from: <http://www.ioffe.ru/SVA/NSM/Semicond/GaInAs/index.html>

- 
- <sup>18</sup> S. Monaghan, É. O'Connor, I. M. Povey, B. J. Sheehan, K. Cherkaoui, B. J. A. Hutchinson, P. K. Hurley, F. Ferdousi, R. Rios, K. J. Kuhn, and A. Rahman, *J. Vac. Sci. Technol. B*, **31**, 01A119, (2013).
- <sup>19</sup> D. Varghese, Y. Xuan, Y. Q. Wu, T. Shen, P. D. Ye, and M. A. Alam, *Proc. IEEE Int. Electron. Devices Meet.*, p. 379, (2008).
- <sup>20</sup> A. Ali, H. Madan, S. Koveshnikov, S. Oktyabrsky, R. Kambhampati, T. Heeg, D. Schlom, and S. Datta, *IEEE Trans. Electron Devices*, **57** (4), p. 742, (2010).
- <sup>21</sup> H.-P. Chen, Y. Yuan, B. Yu, J. Ahn, P. C. McIntyre, P. M. Asbeck, M. J. W. Rodwell, and Y. Taur, *IEEE Trans. Electron Devices*, **59** (9), p. 2383, (2012).
- <sup>22</sup> E. O'Connor, K. Cherkaoui, S. Monaghan, B. Sheehan, I. M. Povey, and P. K. Hurley *Microelec. Eng.*, **147**, p325 (2015).
- <sup>23</sup> E. Nicollian, J. Brews, *MOS Phys. and Tech.*, Wiley, (1982).
- <sup>24</sup> Y. Yuan, L. Wang, B. Yu, B. Shin, J. Ahn, P. C. McIntyre, P. M. Asbeck, M. J. W. Rodwell, and Y. Taur, *IEEE Elec. Dev. Lett.*, **32**, p485, (2011).
- <sup>25</sup> V. Djara, K. Cherkaoui, M. Schmidt, S. Monaghan, É. O'Connor, I. M. Povey, D. O'Connell, M. E. Pemble, and P. K. Hurley, *IEEE Trans. Elec. Dev.*, **59**, 1084, (2012).